

rounding medium,  $n_1$ . Should it be, however, otherwise (direction of dark colour displacement opposite to that of the birefringent prism shift), refractive index of the object under investigation will have to be considered as being lower ( $n$  less than  $n_1$ ).

### 1.2. Uniform Colour Method with High Image Shearing Effect (Prism No. 3)

In this method, it is recommended to observe the sequence of darkenings for images being split during transversal shift of the birefringent prism in order to estimate the magnitude of refractive index for the object under investigation.

If the sequence of image darkening by a dark colour of the zero interference order is consistent with the direction of shift, refractive index  $n$  of the object under observation will be higher than that of the surrounding medium,  $n_1$ , and vice versa, where the sequence of image darkening by such a dark colour remains in opposition to the direction of prism displacement the refractive index  $n$  will be lower than  $n_1$ .

### 1.3. Fringe Method (Prism No. 2)

While shifting the birefringent prism one must notice the side of an interference order zero fringe on which darkening of one or the other image of the object under observation starts to proceed. If the L.H. image darkens on the R.H. side of such a fringe and the R.H. image on L.H. one, refractive index  $n$  of the object will remain higher than  $n_1$  of the surrounding medium, and vice versa, if the L.H. image darkens on the L.H. side of the dark zero image and the R.H. image on R.H. side of this fringe the refractive index  $n$  will be lower than  $n_1$ .

All the above discussed combinations have been listed in Table III and from its data one can easily find out whether refractive index of the object under observation is higher or lower than that of the surrounding medium.

## 2. ASSESSMENT OF SURFACE MICRO-IRREGULARITIES

Assume a transparent slide with some microscopic irregularity of the surface. The examination is to find out if we have to do with a concave or convex irregularity.

A qualitative observation of the microscopic image will be not sufficient enough to say something more certain about such an irregularity since one and the same detail often happens to look once as a hill and soon afterwards as a valley. Moreover, in one interference colour it will make an impression of a hill and in an other one of a valley.

However, the interference methods enable the examiner to state beyond any doubt if he has to do with a convey of concave detail of an object. He must only know that refractive index  $n$  of the slide under examination is higher or lower than that  $n_1$  of the medium overlying such a slide. Then, by observing the direction of dark colour moving within the image of detail being analysed (differential method), or by noticing succession in which split images (the uniform colour method with a high image shearing effect and the fringe method) will go out it will be possible to check in a similar manner as before in the event of refractive index assessment what the nature of microirregularities observed can be. For various variants of each of the methods refer to Table III.

## 3. MEASUREMENTS OF THE REFRACTIVE INDEX AND THICKNESS USING INTERFERENCE FRINGE METHOD AND THE METHOD OF UNIFORM FIELD WITH HIGH IMAGE SHEARING EFFECT (i.e. PRISMS NOS. 2 and 3)

Having measured in accordance with the foregoing description optical path difference  $\phi$  of an object under investigation in relation to the surrounding medium of a known refractive index  $n_1$ , the operator is in a position to find from the formula:

$$\phi = (n_1 - n)t \quad (22)$$

what the refractive index  $n$  of such an object is provided thickness  $t$  of this object is known, and vice versa, he will be able to determine thickness  $t$  if he only knows refractive index  $n$  (Fig. 30),  $\phi$  being positive (+) for  $n < n_1$  and negative (-) for  $n > n_1$ . In order not to commit an error it would be advisable, therefore, to use the previously described procedure for knowing whether the refractive index  $n$  of the object under examination remains higher ( $n > n_1$ ) or lower ( $n < n_1$ ) than  $n_1$  of the surrounding medium. Should the measurement of optical path difference be conducted in two immersion media (e.g. in the air and in water, or in the water and some other liquid) of known refractive indices  $n_1$  and  $n_2$ , it would be possible to determine at a time both refractive index  $n$  of the object being examined and its thickness  $t$ . Two equations would be involved under such circumstances, notably:

$$\phi_1 = (n_1 - n)t \quad (23)$$

$$\phi_2 = (n_2 - n)t$$

to find  $n$  and  $t$  in the following way:

$$n = \frac{\phi_1 n_2 - \phi_2 n_1}{\phi_1 - \phi_2} \quad (24)$$

$$t = \frac{\phi_1 - \phi_2}{n_1 - n_2} \quad (25)$$

whereby optical path differences  $\phi_1$  and  $\phi_2$  have to be considered as positive (+) or negative (-), this in conformity with the aforementioned rule.

The double immersion method can only be used when object under investigation behaves in one and the same manner in both media. Immersion liquids must be chosen, therefore, so that no change takes place in both thickness and refractive index of the object being examined.

Another method for a simultaneous measurement of thickness and refractive index includes optical path difference being measured for two different light wavelengths  $\lambda_1$  and  $\lambda_2$ . This method can be, however, utilized only when immersion medium shows high dispersion of the refractive index as compared to that of the investigated object. In such a case, there are two equations analogous with those given in (23) where  $n_1$  and  $n_2$  represent known refractive indices of the surrounding medium, related to wavelengths  $\lambda_1$  and  $\lambda_2$  respectively. Cinnamon oil is just the liquid exhibiting such a high dispersion of refractive index.

Yet another method of a simultaneous measurement of the refractive index and thickness consists in the measuring of optical path difference at two different temperatures at which a great change takes place in refractive index of the surrounding medium while refractive index and thickness of the object under investigation remain unchanged or undergo a very small change only.

From Formula (22) it is evident that in order to evaluate refractive index  $n$ , of an optional immersion medium one must know thickness  $t$  and refractive index  $n$  of any standard reference object (e.g. thin and narrow glass plate).

#### 4. MEASUREMENT OF REFRACTIVE INDEX BASED ON THE DIFFERENTIAL INTERFERENCE METHOD (PRISM No. 1)

Let us consider any optional object  $B$  of a mild optical path difference gradient (Fig. 31). If the tangential angle  $\alpha$  at any chosen point  $H$  within this object is known, then by measuring in the previously described manner optical path difference  $\Psi$  between the interfering wa-

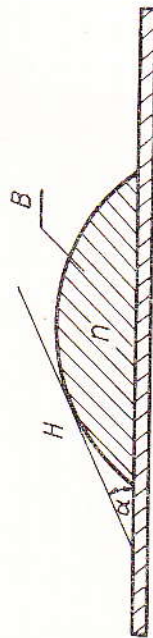


Fig. 31

ves within the interference image of such a point we can arrive at refractive index  $n$  of the object  $B$  by adopting the following formula (13):

$$\tan \alpha = \frac{\Psi}{r(n_1 - n)}$$

where:

$n_1$  — known refractive index of surrounding medium;  
 $r$  — image shearing value;

the value of  $\Psi$  in said formula is to be considered as being positive (+) if  $n_1 > n$ , and negative when  $n_1 < n$ .

If the optical path difference  $\Psi$  at any chosen point of the object under observation is measured in two different immersion media having known refractive indices  $n_1$  and  $n_2$ , it will be possible then to determine both tangential angle  $\alpha$  and refractive index  $n$ .

We have under such circumstances two equations:

$$\tan \alpha = \frac{\Psi_1}{r(n_1 - n)} \quad (26)$$

$$\tan \alpha = \frac{\Psi_2}{r(n_2 - n)}$$

from which  $n$  can be derived in the following manner:

$$n = \frac{\Psi_2 n_1 - \Psi_1 n_2}{\Psi_2 - \Psi_1} \quad (27)$$

and so the angle  $\alpha$  can be had from one of the equations (26). Optical path differences  $\Psi_1$  and  $\Psi_2$  in equations (26) and (27) are to be regarded as positive (+) or negative (-) according to the rule as given above. To achieve a better accuracy of measurement for the refractive index  $n$ , the measurement is advised to be taken at more than only one point with an average value adopted as the final result. Immersion liquids are to be chosen so as to preserve optical and geometrical features of the object completely unchanged.

In addition to the double immersion method also in this case the previously discussed methods of two different light wavelengths and two different temperatures can be employed.

To facilitate the measurement of refractive index in liquids by means of a differential prism (No. 1) special refractometric vessels have been designed, available as optional items. Such a refractometric vessel consists of a basic glass object slide  $SP$  (Fig. 32) to which refractometric plate proper,  $PR$ , having an oblique step and an auxiliary plate  $PP$  are attached. Between these plates a narrow passage is provided to insert a droplet of the liquid  $C$  under investigation and to cover it with a microscopic slip  $SN$ .

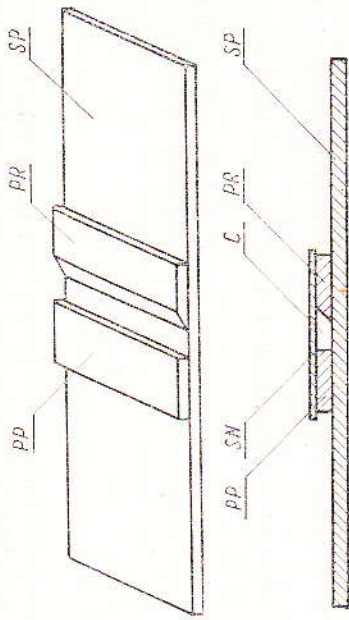


Fig. 32: Cell for measuring refractive index of liquids by a method of differential interference  
 PR — Refractometric plate; PP — Auxillary plate; SP — Microscopic slide; SN — Microscopic cover slip; C — Liquid under examination

By measuring optical path difference within the interference image area of the oblique step one can find refractive index  $n_1$  of the liquid C from the following formula:

$$n_1 = n \pm \frac{\Psi}{\tau \cdot \tan \alpha} \quad (28)$$

where:

- $n$  — known refractive index of the refractometric plate PR;
- $\alpha$  — angle of oblique step in this plate ( $\alpha = 45$  deg.)
- $\tau$  — image shearing depending on objective magnifying power (see Table II).

In formula (28) sign "+" applies to  $n_1$  greater than  $n$  and "-" to  $n_1$  smaller than  $n$ .

The measurement is taken by means of a  $\times 10$  objective. Refractometric vessels are located on the microscope stage so that the upper edge of PR plate step be disposed centrally versus the microscopic field of view and parallelly versus refracting edge of the birefringent prism. So, the field of view remains divided into two equal portions, portion I and II (Fig. 33), having different shades if the white light has been employed, or different brightness if monochromatic light has found use.

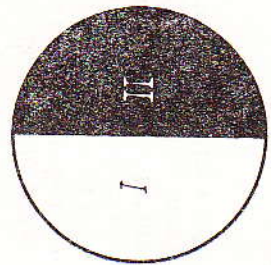


Fig. 33: Field of microscopic view while measuring refractive index by means of a refractometric cell as shown in Fig. 32

Optical path difference  $\Psi$  measurement takes place in the uniform dark colour of a zero interference order, with a maximum darkening of the two halves of said field of view done in succession, or by establishing the same level of brightness for both these halves. In the first case, the optical path difference can be had from the formula:

$$\Psi = (p_1 - p_0) \frac{\lambda}{h} \quad (29)$$

and in the other, from the formula:

$$\Psi = 2(p_r - p_0) \frac{\lambda}{h} \quad (30)$$

where:

$p_0$  — represents zero position of the birefringent prism, in which maximum darkening of one half field of view providing an image of the refractometric plate behind the step takes place,

$p_1$  — represents position of the birefringent prism in which maximum darkening of the second half field of view providing step image takes place,

$p_r$  — represents position in which both halves of the field of view take on an identical level of brightness.

Both halves can be set for an identical brightness only when the optical path difference  $\Psi$  becomes smaller than the applied light wavelength. Setting for a maximum darkening of first one and then also the second half field of view will depend on the visual perception to notice the maximum darkening of the image.

A more reliable setting of the birefringent prism can be had by observing differential image formed in the focal plane of an objective. To this end, an auxiliary microscope must be put in place of one eyepiece of the binocular attachment to be focused in the plane of objective exit lens where two images  $S_0$  and  $S_1$  (Fig. 34) of the slit S

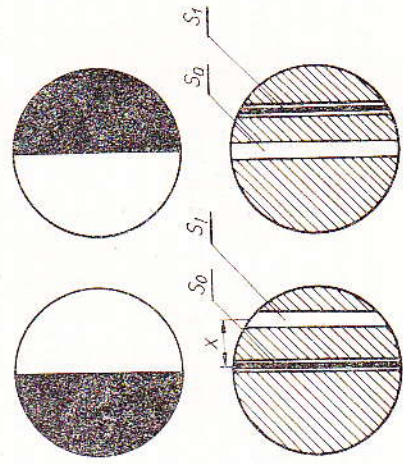


Fig. 34: Refractive index measured in liquids by the differential interference method using refractometric cell as shown in Fig. 32

(Fig. 1) can be seen at a time. By shifting birefringent prism in the required direction it must be brought into such a position where a zero interference fringe could pass centrally through one and then also the second image of the slit. Such a position corresponds to the maximum darkening of the first and then also the second half field of view, and is deprived of the uncertainty which assessment of the maximum darkening includes in itself. A precise central positioning of the zero interference fringe just in the middle of images  $S_0$  and  $S_1$  appears to be highly sensitive and guarantees an accuracy of 0.01 mm in the birefringent prism setting, and 0.0001 in the refractive index measurement. Separation  $x$  between slit images  $S_0$  and  $S_1$  increases right with the amount of difference between refractive indices of the investigated liquid and refractometric plate. If this difference is small enough, a measurement with the aid of this method becomes impossible since images  $S_0$  and  $S_1$  of the slit coincide with each other.

There are two refractometric vessels in all. They differ in refractive indices  $n$  of their refractometric plates  $PR$ . The two vessels form a set by means of which one can measure refractive index within the 1.3 to 1.8 interval.

##### 5. MEASUREMENT OF REFRACTIVE INDEX BY THE DIFFERENTIAL INTERFERENCE FRINGED FIELD METHOD (PRISM No. 2)

Refractive index of liquids when measured by the differential interference fringed field method (prism No. 2) requires the use of refractometric vessels as referred to above.

Refractive index for liquids can be had from the formula 28. Optical path difference in formula 28 can be calculated, on the other hand, from formula 15 by measuring an inter-fringe spacing  $h$  (as described in Chapter 5) with the aid of an  $\times 12$  micrometer eyepiece and by finding interference fringe deviation  $d$  (preferably zero fringe) within the skew step area.

An  $\times 10$  objective will suit best for that type of measurement. The refractometric vessel must be arranged on the microscope stage in such a way as to have upper edge of the refractometric  $PR$  plate step (Fig. 32) in parallel configuration with interference fringes observed in the microscopic field of view.

Then, mechanical stage of the microscope must be adjusted so as to bring refractometric vessel in perpendicular alignment with the interference fringes, but outside the oblique step, and position of the dark zero fringe established by means of micrometric scale eyepiece. After a reading has been taken from the eyepiece scale, oblique step of the refractometric plate  $PR$  should be focused in the field of view to read next displacement  $d$  of the zero fringe. If the zero fringe displacement occurs towards the liquid under investigation, refractive index  $n_1$  will be less than  $n$  and consequently also a negative value of  $\Psi$  must be

used in formula 28. If, on the other hand, interference fringes move towards refractometric plate, refractive index  $n_1$  will be greater than  $n$  and a positive value of  $\Psi$  must be applied to the formula. In this latter case, zero fringe can be observed in the microscopic field of view — within the oblique step area and beyond it, at the same time.

For a definite constant position of prism  $W_1$  under its vertical adjustment, and for a specified refractometric plate, terms  $\frac{1}{r \cdot \tan \alpha}$  (in formula 28) and  $\frac{\lambda}{h}$  (in formula 15) will remain constant and so the formula 28 can be written, as follows:

$$n_1 = n \pm K \cdot d \quad (28a)$$

where  $K$  represents a constant value to be easily determined by measurement of the interference fringe deviation for a kind of liquid of a known refractive index  $n_1$  and for a fixed, preferably the highest and lowest, position of prism  $W_1$ . To improve accuracy, two or three standard liquids can be introduced. Practically, calibration of the microscope (determination of constant  $K$ ) can be presented in the form of a diagram where refractive indices of the two or three liquids used in the process are plotted under a rectangular coordinate system against the value of zero fringe displacement effected within the refractometric plate oblique step area.

As to be seen from formula 28 relationship thus obtained will represent a straight line intersecting the axis of refractive indices at a point  $n$  corresponding to the actual value of refractive index for the refractometric plate in use.

In some cases when dispersion factor of the liquid greatly differs from that of the refractometric plate, the deviated dark zero fringe may have a hue making its identification more difficult.

In such circumstances, to distinguish univocally which deviated fringe corresponds to a non-deviated zero fringe the refractometric vessel must be positioned so as to bring its oblique step edge into perpendicular alignment with the interference fringes, then, it will be necessary to rotate the stage slowly to see which one from the fringes dislocating within the area of said oblique step will join with the dark zero fringe non deviating in the area outside the oblique step.

In such a way, the deviated zero fringe can be easily and accurately identified and this represents an important feature of the method under consideration.

## MEASUREMENT OF BIREFRINGENCE

## 1. FRINGED FIELD MEASUREMENT (PRISM No. 2)

Let us consider any plano-parallel birefringent plate, no matter what its shape, cut out parallelly to the optical axis (Fig. 35).

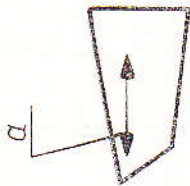


Fig. 35: Birefringent plate  
a — direction of optical  
axis

Such a plate when viewed through a polarizing interference microscope, using the interference fringed field method, will behave differently compared to an isotropic one. Basic difference is that observed in the non-split portion of the image. A plano-parallel isotropic plate would produce no change of the interference field in this portion of the image whereas a birefringent plate could exhibit such a behaviour only if the direction of its optical axis had formed an angle of  $45^\circ$  versus that shown by interference fringes (Fig. 36). There are four such positions available. While rotating microscope stage together with the plate through  $360^\circ$ , the situation will repeat itself at  $90^\circ$  intervals, i.e. every ninety degrees of rotation.

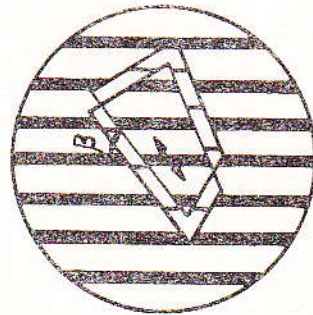


Fig. 36: Birefringent plate in a fringed interference field with its optical axis set an angle of  $45^\circ$  versus the direction of interference fringes

By measuring in one of these positions angle  $\beta$  formed between the direction of interference fringes and any freely chosen edge of the plate one can determine the direction of light oscillation within a birefrin-

gent plate which direction is that of the optical axis and this at right angles thereto. In any other position of the plate, displacement of interference fringes takes place in the non-split portion of the image. If the direction of optical axis in the plate remains parallel or perpendicular versus that of interference fringes (Fig. 37), contrast of the deviated fringes will reach its maximum level. Fringes deviated within a non-split image of the plate do vary in nothing from relevant fringes in the remaining field of view. This creates a situation in which direction of the optical axis can be found with ease also in the birefringent objects. White light is the most convenient source of radiation in this specific case. The recommended procedure consists in such a manipulation of the rotary microscope stage with the object under examination provided thereon that fringes being deviated in a non-split area of the produced image might arrive at the maximum possible contrast and tint identical with that of relevant fringes seen in the field of view.

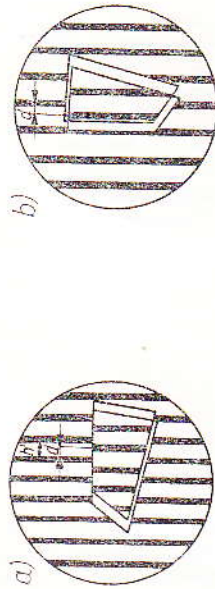


Fig. 37: Birefringent plate in a fringed interference field in perpendicular (a) and parallel (b) alignment versus interference fringes and birefringence measured by establishing deviation  $\alpha$  of fringes

Should the investigated object be positive ( $n_e$  being larger than  $n_o$ ) from the birefringent viewpoint, and should fringes deviate in the right-hand direction (Fig. 37a), then the direction of optical axis in such an object will have to be considered as being at right angles to that of the interference fringes. Should, on the other hand, fringes deviate in the left-hand direction, then the direction of optical axis will have to be considered as being parallel towards that of the interference fringes (Fig. 37b). A reverse situation prevails in the event of negatively birefringent objects ( $n_e$  smaller than  $n_o$ ).

By positioning a birefringent plate with its optical axis being perpendicular or parallel towards the direction of interference fringes (Fig. 37), and by measuring in one of these positions the amount of deviation from a dark zero fringe, one can easily find birefringence

$n_e - n_o$  of the examined plate, if he only knows its thickness  $t$ , from the formula as follows:

$$\delta = (n_e - n_o) t = \frac{d}{h} \cdot \lambda \quad (31)$$

where:

- $n_o$  — ordinary refractive index;
- $n_e$  — extraordinary refractive index;
- $t$  — plate thickness;
- $h'$  — inter-fringe spacing;
- $\lambda$  — applied light wavelength.

Optical path difference  $\delta$  due to birefringence can also be found using the method of a transverse shift of the birefringent prism. For this purpose, the birefringent prism producing a fringed field must be brought to such a position  $p_0$  in which dark zero fringe in the field of view will intersect by a straight line with a specified point  $B$  of the image under observation (Fig. 38a). Further on, the same birefringent

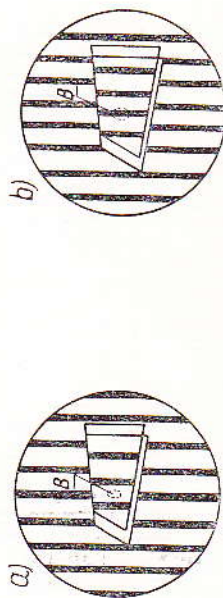


Fig. 38: Birefringence measured in the fringed interference field by displacement of the birefringent prism

prism must be brought to such a position  $p_1$  in which the same zero interference fringe will pass through the chosen point  $B$  (Fig. 38b).

Optical path difference  $\delta$  can be found from the formula:

$$\delta = (p_1 - p_0) \cdot \frac{\lambda}{h} = (n_e - n_o) \cdot t \quad (32)$$

wherein  $h$  is the true inter-fringe spacing for a birefringent prism (Table II, Prism No. 2). This method is suitable for measuring very large optical path differences  $\delta$  (up to  $20 \lambda$ ) accurate to an order of  $\lambda/20$ .

The ordinary refractive index  $n_o$  and the extraordinary one  $n_e$  can be found by positioning the plate so as to make the direction of its optical axis once parallel and then perpendicular towards that of light oscillations in the polarizer (Fig. 39).

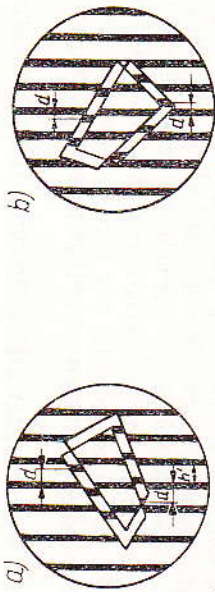


Fig. 39: Ordinary and extraordinary index of refraction for a birefringent plate measured in a fringed interference field by establishing deviation  $d$  of fringes

By measuring in both cases deviation  $d$  of the zero fringe within the split portion of image one can evaluate optical path difference  $\phi$  for the ordinary and extraordinary ray from the formula:

$$\phi = \frac{d}{h} \lambda \quad (33)$$

If we know thickness  $t$  of the plate at the point where optical path difference  $\phi$  has been measured, it will be possible to find  $n_o$  or  $n_e$  from the formula:

$$\frac{d}{h'} \cdot \lambda = (n_{oe} - n) \cdot t \quad (34)$$

where:

- $n$  — refractive index of medium surrounding the plate;
- $n_{oe}$  — refractive index of the ordinary or extraordinary ray.

As the optical path difference  $\phi$  in two media having known refractive indices  $n_1$  and  $n_2$  has been measured, it will be possible to find at a time also refractive indices  $n_o$  and  $n_e$  and the thickness  $t$ .

If a birefringent prism, which is optically inactive, has been cut out at right angles to the optical axis, then its behaviour will resemble this of an isotropic plate and only the ordinary refractive index  $n_o$  will be measured in these circumstances. On the other hand, a thin birefringent plate cut out in parallel to the optical axis will behave like a birefringent plate cut out in parallel to the optical axis, with the only difference that birefringence of such a plate will be smaller since refractive index for an extraordinary ray does not have an extreme value in such a case.

If a birefringent plate which has been cut out in parallel with the optical axis is disposed so that the direction of optical axis remains parallel or perpendicular towards this of light oscillations in a polarizer, then no change will occur in the colour of field background to the non-split image of such a plate. During one full rotation of the stage there will be four such positions, therefore, in which a birefringent plate in a not-split area of the image will adopt an identical tinge as the field-of-view background. These positions are being called positions of extinction.

In any other position, which does not coincide with that of extinction, plate image will receive another colour (or brightness if a monochromatic light is applied) whereby the same change in colour will occur four times during a full rotation of the stage. Should, however, the birefringent plate be moved through  $45^\circ$  together with the microscope stage from any freely chosen position of extinction in either direction (depending on whether optical axis of the plate remains perpendicular or parallel towards refracting edge of the birefringent prism), then the colour of image will resolve itself into any initial tinge of the field-of-view background.

An absolute difference in  $p_0$  and  $p_1$  positions of a birefringent prism, in which field-of-view background and then also a non-split image of the birefringent prism will adopt the same colouration, is right the measure of birefringence  $n_e - n_o$  for the plate under examination:

$$\delta = (p_1 - p_0) \cdot \frac{\lambda}{h} = (n_e - n_o) \cdot t \quad (35)$$

where  $t$  represents plate thickness.

With the aid of a differential prism No. 1 one can use this method to measure birefringence only, but when use will be made of prism No. 3 providing a high image shearing effect both birefringence as well as the ordinary and extraordinary refractive indices will be measured.

Said refractive indices are being measured in the split portion of image while the birefringent plate is set in two adjacent position of extinction. Further procedure will be similar to that described above for isotropic objects.

An optically inactive birefringent plate cut out at right angles to the optical axis exhibits in an uniform interference field similar properties as the isotropic plate whereas a thin plate cut out obliquely towards optical axis will behave identically as a plate cut out in parallel to this axis.

## MEASUREMENT OF LIGHT TRANSMITTANCE

The polarizing interference microscopy can be used not only for the examination of completely transparent phase objects, but also for the observation of amplitude or — more generally speaking — phase-amplitude objects which absorb to some extent light rays. With regard to such objects, the polarizing interference microscope may perform the function of a microphotometer to measure both the transmittance of light passing through the object and phase displacement, at the same time.

The measurement can be carried out in a uniform interference field as well as in a fringe field with a high image shearing effect where the most convenient practice includes the use of a dark colour or a dark zero fringe (zero interference order).

Assume that the engaged prism No. 3 has been set for a uniformly dark colour of the field-of-view background. The phase-amplitude object absorbing to some extent light rays and having its transverse dimensions smaller than image shearing value  $\tau$  can under these circumstances be seen in the form of two bright separated images (Fig. 40a) similarly to a completely transparent purely phase object.

When shifting birefringent prism in either direction first one and then also the second image (Fig. 40b, c) is darkened. This is, however, not the maximum darkening since amplitudes of the interfering waves, because of light being absorbed by the object under observation, remain not identical within the area of image shearing. To obtain equalization of amplitudes in either of the images, along with their maximum darkening (Fig. 40d, e), the polarizer must be turned in this or another direction (from the position of having been crossed with the analyser) through an angle  $\gamma$ . This angle is used to measure light transmittance  $P$ :

$$P = \tan^2(45^\circ - \gamma) \cdot 100\% \quad (36)$$

When darkening one and the same area in the two successively following images of the object under observation, the angle of polarizer rotation should, in principle, remain the same. Considering this fact, it would be advisable so far as possible to measure light transmittance on both images with the mean value of two such measurements taken as the final result. The procedure should be then as follows.

With the crossed polarizer and analyser, birefringent prism must be moved in the transverse direction so as to darken one of the images (Fig. 40b); then, by twisting polarizer in respective direction it must be brought into such a position  $\gamma_1$  in which the image gets maximum darkening (Fig. 40d). This position can be read from angular scale whereas original position of the polarizer is to be restored (Fig. 40b). By

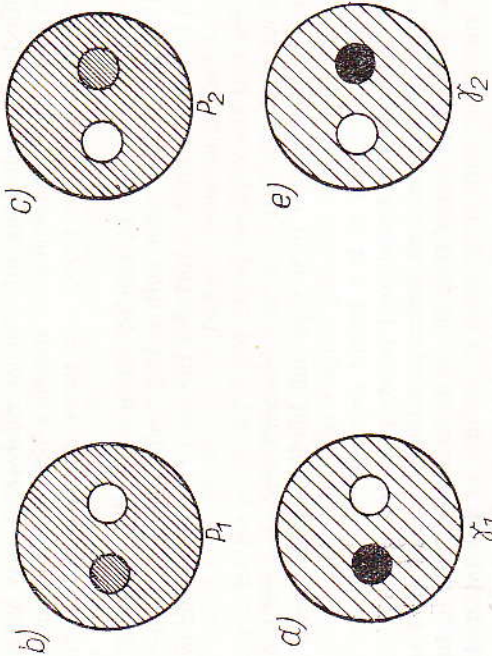
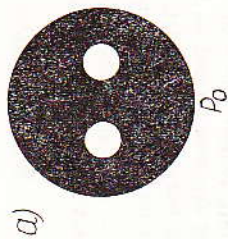


Fig. 40: Simultaneous measurement of optical path difference and light transmittance  
 a) Zero position of birefringent prism; b) Compensation of phase shift in L.H. image; c) Compensation of phase shift in R.H. image; d) L.H. image amplitude compensation; e) R.H. image amplitude compensation

shifting birefringent prism in the opposite direction extinction of the second image (Fig. 40c) takes place to yield next to the maximum darkening effect like in the previous step caused by rotation of polarizer in the reverse direction. In this position of the polarizer another reading, referred to as  $\gamma_2$  (Fig. 40e), is to be taken. The difference of  $\gamma_2 - \gamma_1$  when divided by two gives angle  $\gamma$ ; by substituting this in formula (36) transmittance  $P$  can be derived.

Suppose, for instance, that  $\gamma_1 = 29^\circ$  and  $\gamma_2 = 60^\circ$ , then....

$$\gamma = \frac{\gamma_2 - \gamma_1}{2} = \frac{31}{2} = 15.5^\circ$$

in other words  $P = \tan^2(45 - 15.5)100\% = \tan^2 29.5^\circ \cdot 100\% = 23\%$ .

If we take during this operation readings for prism positions  $p_1$  and  $p_2$ , responsible for the maximum darkening of images, it will be then

possible to measure also phase displacements of the light wave passing through the object under observation.

Whenever prism No. 2 is used to produce fringed field, a similar procedure will be adopted to measure transmittance, i.e. with the crossed analyser and polarizer first one and then the second image remains darkened with the zero interference fringe after a previous maximum extinction of the image caused by adequate rotation of the polarizer.

So far, it has been assumed that images of the object remain completely separated. Of course, a complete separation of the images is required only with regard to optically heterogeneous areas lacking uniformity in both phase displacement and amplitude of the incident light wave. On the other hand, in the event of such homogeneous objects like e.g. thin layers, plates or films this requirement must not necessarily be met, and only a partial splitting of the images will suffice. In such circumstances, it is possible to conduct measurements of both transmittance as well as phase displacement on the three fundamental types of samples, i.e. on a sill (Fig. 23), step (Fig. 24) and groove (Fig. 25). The least required among these samples is "step" since measurements can be taken in this case on one image only. In such a situation, highest accuracy must be applied to determine crossed position of the polarizer in which maximum darkening of the field-of-view background is produced. This position may slightly differ from that referred to on the angular polarizer scale as division 45 or 135, marked by a red cross. The instance covering such a type of image can be, however, resolved into this of two images if only mechanical stage of the microscope is moved through 180 deg. together with the specimen.

One of the positions will then yield an ordinary image, and the other an extraordinary one. This procedure is, however, possible only under a uniform colour method technique (prism No. 3); attention must be, however, given during this technique that fragment of the object being viewed has always one and the same position in the field of view.

#### Angle of Polarizer Rotation

Polarizer (Fig. 13) has an angular scale 19 with incisions made every 5 degrees and marked in both opposite directions from  $0^\circ$  up to  $180^\circ$ . A two sided nonius 20 and 21 ensures an accuracy of  $1^\circ$  for the angular setting readings. Polarizer rotations, accurate to  $5^\circ$ , can be read from the angular scale according to marker  $\blacktriangledown$  indications whereas those accurate to  $1^\circ$  from nonius 20 or 21 according to whose elementary divisions starting from marker  $\blacktriangledown$  are on the rising side of angular scale 19.

And so, for instance, polarizer in Fig. 13 has been set to  $45^\circ$  since the angular scale reading is  $45^\circ$  (marker  $\blacktriangledown$  comes after  $45^\circ$ ) and in the left-hand nonius 20 (this is exactly the nonius whose graduations are on the rising side of angular scale 19) it is the fifth mark which coincides with the line of scale 19.

## ESTIMATION OF DRY MASS IN LIVING CELLS

Let us assume that a biological cell can be seen as a homogeneous plate of thickness  $t$  (Fig. 30) immersed in an aqueous medium. In this cell, optical path difference  $\phi_w$  between the incident beam of light that passes through the cell and this passing beyond it will be expressed, as:

$$\phi_w = (n_w - n)t \quad (37)$$

where:

$n$  — refractive index of the cytoplasm,

$n_w$  — refractive index of water.

On the other hand, the following relationship exists between refractive index  $n_w$  of the solvent (water in this specific case) and concentration  $c$  expressed as  $m$  grammes of the cytoplasm dissolved in 100 millilitres of the solution:

$$n - n_w = \delta \cdot c \quad (38)$$

Coefficient  $\delta$ , referred to as specific increment of the refractive index (or specific refractive increment), remains equal to 0.0018 for most biological substances to be met.

Concentration  $c$ , according to the definition given above, can be written as:

$$c = \frac{100 m}{A \cdot t} \quad (39)$$

where  $A$  represents the area of cell projection in a plane at right angles to the direction of incident light beam passing through the cell.

From the above three relationships, one can deduce the following expression for the amount of  $m$  grammes of the dry mass in a living cell:

$$m = \frac{\phi_w \cdot A}{100 \cdot \delta} \quad (40)$$

Hence, by measuring optical path difference  $\phi_w$  in the manner as described above (uniform interference field with a high image shearing effect, or fringed field method), and by knowing from planimetric measurements area  $A$  of the cell, one can use formula (40) to evaluate directly the total amount of dry mass in grammes on a cell submerged in an aqueous medium.

Should the biological specimen under observation have a highly heterogeneous character with different phase shifts occurring at various

points, then the total content of dry mass will have been calculated by summing up particular contents found within different fragments to be considered as being uniform (homogeneous).

In many an instance, and in the comparative research in particular, the knowledge of dry mass  $m$  per unit area will be sufficient:

$$m' = \frac{m}{A} = \frac{\phi_w}{100 \cdot \delta} \quad (41)$$

Whatever is the measurement, it will be solved under such circumstances into a measurement of the optical path difference,  $\phi_w$ . By knowing dry mass content per unit area and thickness of the cell, one is in a position to evaluate concentration  $c$  of the substance contained therein:

$$c = \frac{m'}{t} = \frac{\phi_w}{100 \cdot \delta \cdot t} \quad (42)$$

The thickness of a cell, or any other biological object, can also be found in the manner as described in Chapter 6 by using the double immersion or two light wavelength methods.

Formulae (40), (41) and (42) apply merely to biological specimens immersed in an aqueous medium. When a cell is, however, contained in a non-aqueous medium which does not penetrate into the cell, the dry mass content can be calculated from the following formula:

$$m = \frac{\phi_s \cdot A}{100 \cdot \delta} + (n_s - n_w) \frac{A \cdot t}{100 \cdot \delta} \quad (43)$$

where:

$\phi_s$  — optical path difference of the cell in relation to surrounding medium;

$n_s$  — refractive index of such a medium.

If we want, therefore, to learn dry mass content in a living cell placed under a non-aqueous medium conditions, we must know its thickness  $t$ . Should, however, refractive index  $n_s$  of the immersion medium only slightly differ from this of water,  $n_w$ , then the second term of formula (43) will almost be negligible as compared to the first one. If this is so, cell thickness  $t$  can be taken as an estimated quantity found by some approximation methods (like e.g. by measurement of cell diameter if a cell is more or less spherical in its overall shape).

It is not like that if a cell is penetrated by the medium itself. In such a case, the cell can be treated as an agglomeration of cytoplasm particles uniformly distributed within a confined three-dimensional volume penetrated by the medium in question (Fig. 41a). The optical path difference  $\phi_s$  caused by the entire cell appears then to be equivalent to that likely to be produced on a layer of densely arranged cytoplasm par-

ticles (Fig. 41b) of an area  $A$  identical with this of the entire cell. Let  $n_c$  be refractive index of the cytoplasm particles;  $n_s$  refractive index of the immersion medium;  $t$  geometrical thickness of the cell; and  $f$  this portion of the cell which is free from cytoplasm particles.



Fig. 41

If only water penetrates into cell from the immersion medium, then optical path difference  $\phi_s$  caused by the cell versus the surrounding medium...

$$\phi_s = (n_c - n_s)t(1-f) - (n_s - n_w)t \cdot f \quad (44)$$

On the other hand, formula (38) under these conditions will have the following form:

$$n_c - n_w = \delta \cdot c = \delta \frac{100m}{A \cdot t(1-f)} \quad (45)$$

By joining equations (44) and (45), the following new expressions can be derived for dry mass content in the cell to be penetrated by water from the surrounding medium:

$$m = \frac{A}{100 \cdot \delta} \phi_s + (n_s - n_w) \frac{t \cdot A}{100 \cdot \delta} \quad (46)$$

If, on the other hand, immersion medium as a whole penetrates the cell (i.e. both water and substance dissolved therein), then the optical path difference  $\phi_s$  will be...

$$\phi_s = (n_c - n_s) \cdot t \cdot (1-f) \quad (47)$$

and the following expression will be provided for the dry mass content:

$$m = \frac{A}{100 \cdot \delta} \phi_s + (n_s - n_w) \frac{A}{100 \cdot \delta} (1-f) \cdot t \quad (48)$$

As will be seen, an "effective" knowledge of cell thickness  $t = (1-f) \cdot t$  will be required to evaluate dry mass content in the living cell penetrated by the surrounding medium. This dry mass content can also be found by the double immersion method.

To estimate dry mass content in a living cell into which water only penetrates from the immersion medium, geometrical thickness  $t$  of the cell will be additionally required.

To find optical path difference in cells and similar biological specimens use can be made of both interference fringe method (Prism No. 2)

and the uniform field method with a high image shearing effect (Prism No. 3). Whichever method is to be adopted will depend to a great extent upon the size of object being examined, the required effect of image splitting and experimental data. Two potentials are then possible:

a) either images of the cell (ordinary and extraordinary) will be completely separated (Fig. 42);

b) or images of the cell will remain only partially split (Fig. 43).

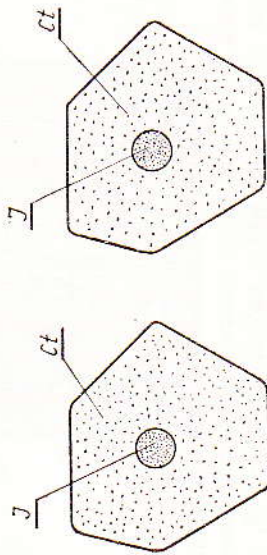


Fig. 42

In case "a" the optical path difference  $\phi_s$  versus immersion medium will be measured at any freely chosen point of the cell whereas in case "b" this measurement will only be made within those areas where no overlapping of the images takes place.

Should we, however, have to do with some nucleated cells, then in the event of partial image splitting, it will be possible to measure the optical path difference of the nucleus in relation to cytoplasm. The image splitting value must then be suited so as to produce split images of the nuclei alone, and to keep same within the limits of a joint area of the cell image (Fig. 43). On the other hand, each time a complete separation of the cell images (Fig. 42) takes place, optical path difference will be measured within the limits of nucleus in relation to the cell sur-

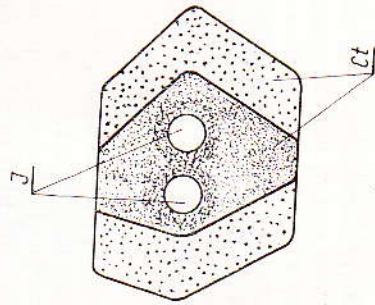


Fig. 43

rounding medium, but including cytoplasm over- and underlying the nucleus, and this is to be taken into account when proceeding with the analysis of a dry mass content in a nucleus.

Let  $\phi_1$  represent optical path difference between cytoplasm  $Ct$  close to the nucleus and medium surrounding the cell (Fig. 44);  $\phi_2$  —

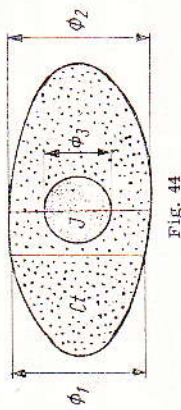


Fig. 44

— optical path difference between nucleus  $J$  in its central part, including cytoplasm overlying and underlying it, and the surrounding medium;  $\phi_3$  — optical path difference between nucleus  $J$  and cytoplasm  $Ct$  surrounding the nucleus. If we ignore possible difference existing in cell thickness at the point where optical differences  $\phi_1$  and  $\phi_2$  have been measured, the following relationship will be true for  $\phi_1$ ,  $\phi_2$ ,  $\phi_3$ :

$$\phi_2 = \phi_1 + \phi_3 \quad (49)$$

Hence,  $\phi_3$  can be had by measurement of  $\phi_1$  and  $\phi_2$ , or  $\phi_2$ , can be derived if we measure  $\phi_1$  and  $\phi_3$ .

The general principles of dry mass estimation, as well as, those for the determination of refractive index and cell thickness, are intended to orient the reader in existing problems and cannot be treated as completely satisfactory. More details and practical hints about same will be found in publications listed at the end of this booklet.

Naturally, the measurements designed to establish dry mass, refractive index and thickness of a cell do not exhaust by any means all the possible applications of a BIOLAR PI microscope in the biological and medical research. Among the numerous other applications there are e.g. such, as the measurement of light transmittance in absorptive micro-objects, measurement of optical path difference gradient and other quantities, investigation of surface tension effects, diffusion tests, analysis of osmotic reactions, measurement of shape in the event of various objects, etc.

In addition, a BIOLAR PI microscopy offers a great number of new interesting potentialities in the field of qualitative tests and observations due in the first place to high plasticity and fidelity in the representation of interference images (differential images in particular), colour contrast adjustment, possibilities of changing over in a continuous manner from colour contrast to a dark or bright field, high sensitivity of interference methods used in this microscope, as well as, possibilities for observation and examination of both amplitude and phase objects.

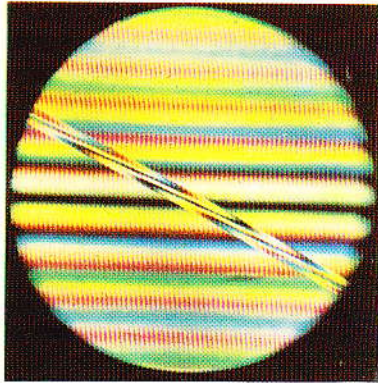
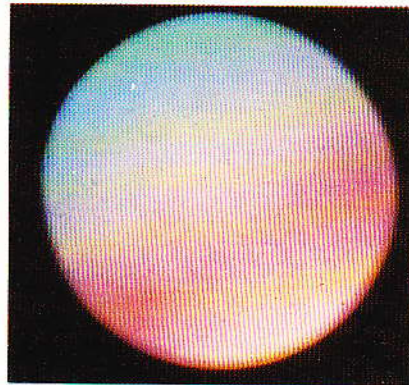
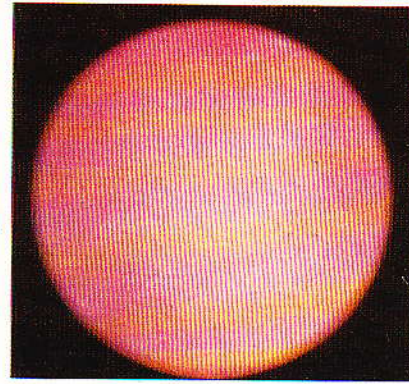


Fig. 45: Fringed interference white light field including a split image of fine Canada balsam fibre immersed in the cedar oil (birefringent prism No. 2;  $\times 10$  objective)



a)



b)

Fig. 46: Polarizing interference microscope adjusted for uniform sensitive colour of the first interference order:

a) Wrong setting; b) Correct setting

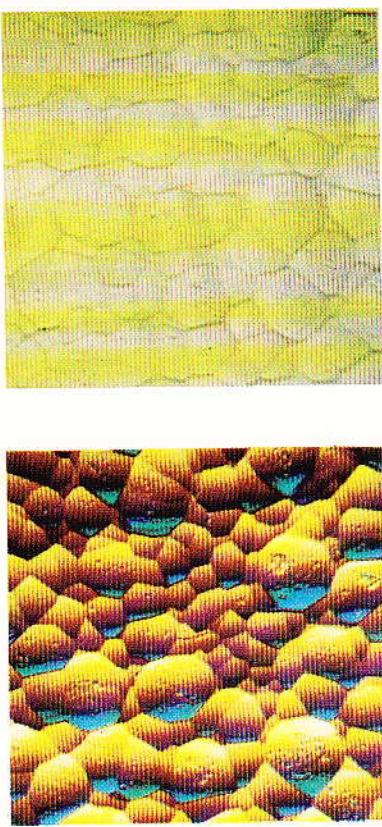


Fig. 48: Image of glass plate surface as etched by hydrofluoric acid and flooded with water:  
 a) As seen in a differential interference field (prism No. 1 set to uniform sensitive colour of the first order); b) As seen in the event of an ordinary bright field microscopy ( $\times 20$  objective)

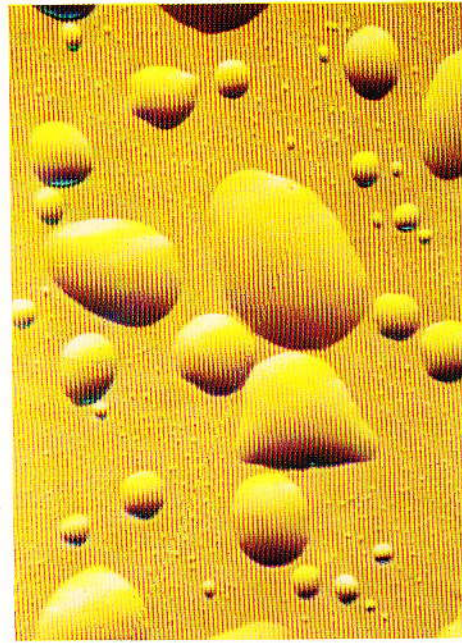


Fig. 49: Cedar oil droplets as seen on a glass slide in uniform yellow-orange colour field of the first interference order — differential method (birefringent prism No. 1;  $\times 20$  objective)

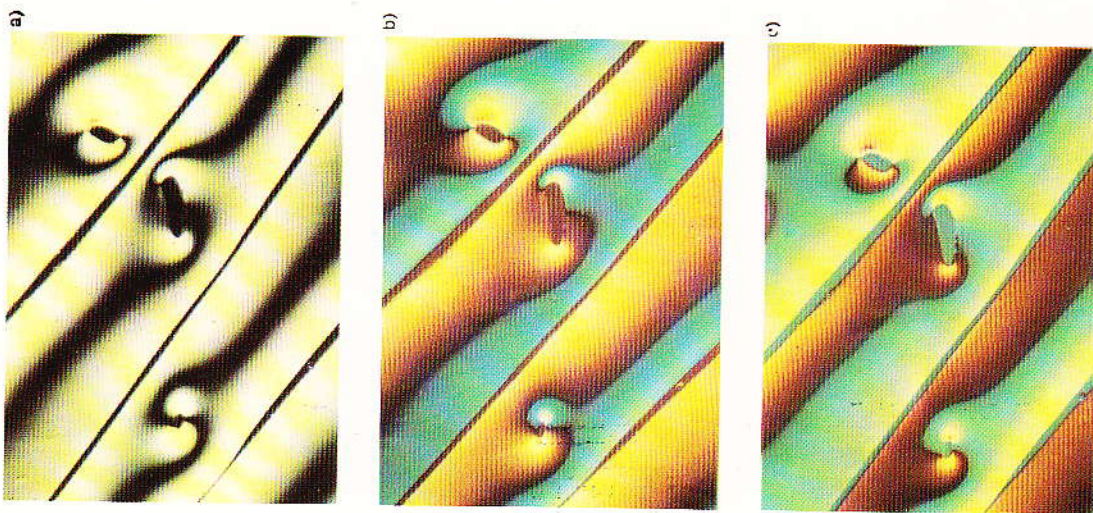
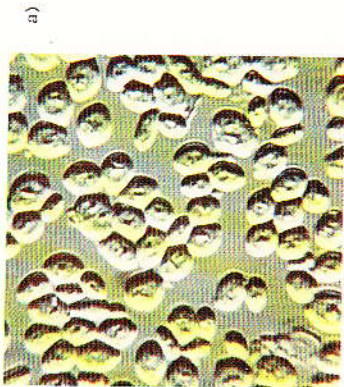
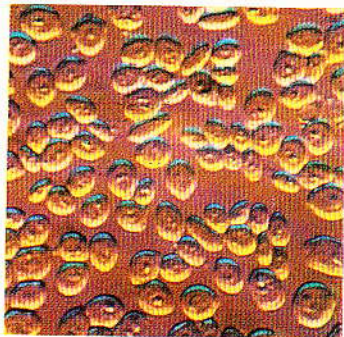


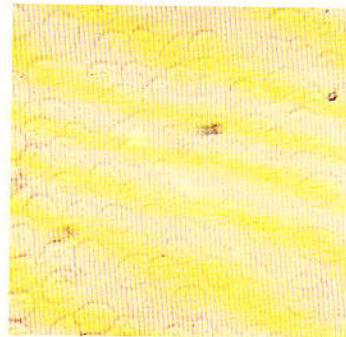
Fig. 47: Image of polyester resin fibre as seen in a uniform interference colour field:  
 a) Dark colour; b) First order purple; c) First order blue — differential method (prism No. 1;  $\times 20$  objective)



a)



b)



c)

Fig. 50: Yeast cells as seen in an aqueous medium

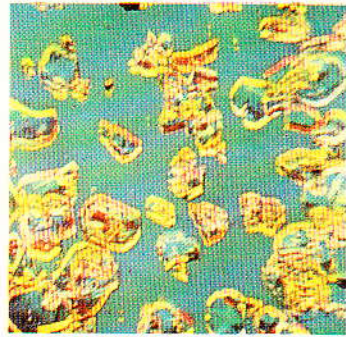
- a) Uniform grey-green colour field of view;  
 b) Uniform sensitive colour of the first interference order (birefringent prism No. 1; X100 immersion objective); c) Ordinary bright field microscopy



a)



b)



c)

Fig. 51: Corundum crystals as seen in a uniform colour field:

- a) Dark colour; b) First order purple; c) First order blue — the method of uniform field with a high image splitting effect (prism No. 3; X100 objective)

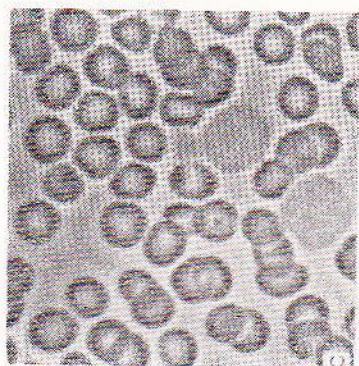
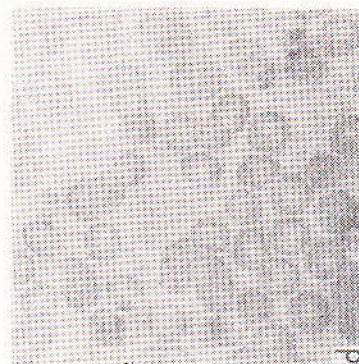
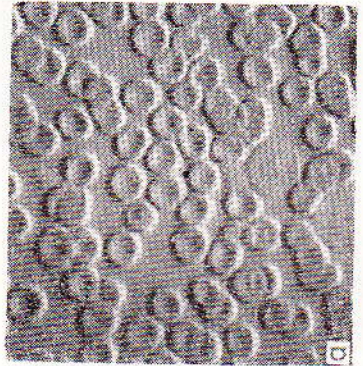
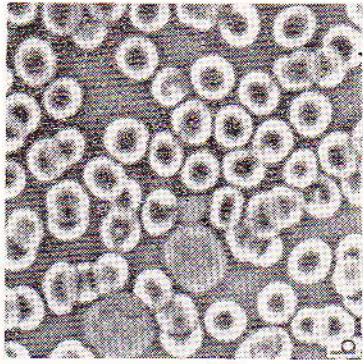


Fig. 52: Blood corpuscles (smear) as seen flooded by a cedar oil  
a) In a uniform differential field (birefringent prism No. 1) polarizing interference microscopy; b) in an anoptical type negative phase contrast microscopy; c) in a positive phase contrast microscopy; d) In an ordinary bright field microscopy with an almost entirely closed iris diaphragm ( $\times 40$  object)

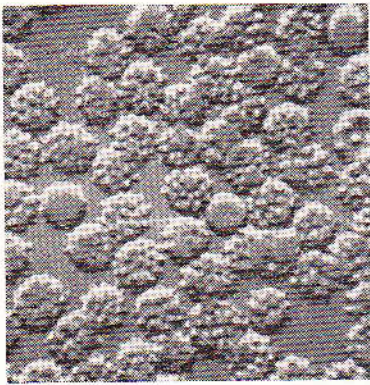


Fig. 53: Red blood corpuscles as seen immersed in an hypertonic aqueous medium through a polarizing interference microscope (uniform differential field method — birefringent prism No. 1)

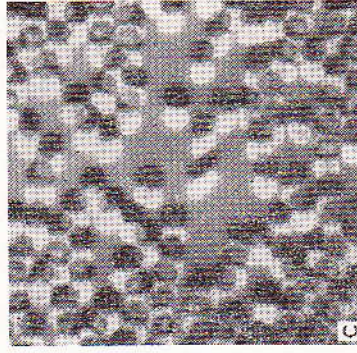
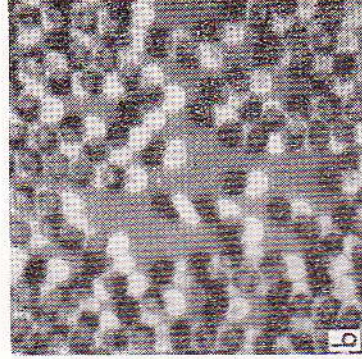
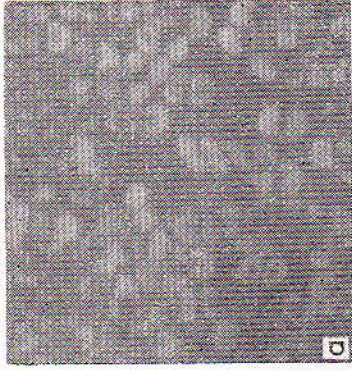


Fig. 55: Red blood corpuscles as seen immersed in cedar oil through a polarizing interference microscope including prism No. 3 (uniform field with a high image shearing effect). Optical path difference measured by darkening images split ( $\times 20$  objective)

a) Birefringent prism set for a dark field of view; b) Maximum darkening of R.H. image of corpuscles; c) Maximum darkening of L.H. image

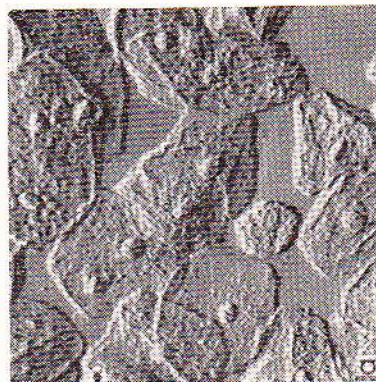
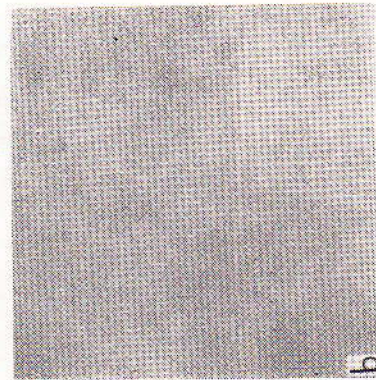


Fig. 54: Epithelial cells from a lip as seen immersed in saliva  
a) Uniform differential field polarizing interference microscopy (birefringent prism No. 1); b) Ordinary bright field microscopy ( $\times 20$  objective)

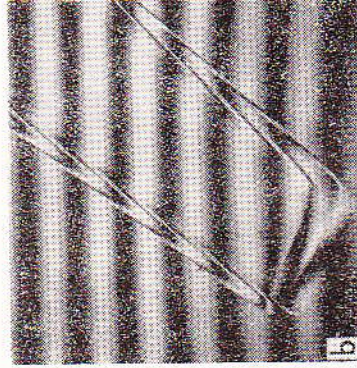
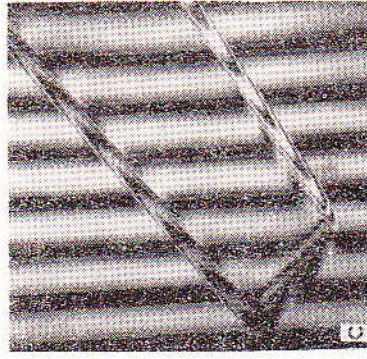
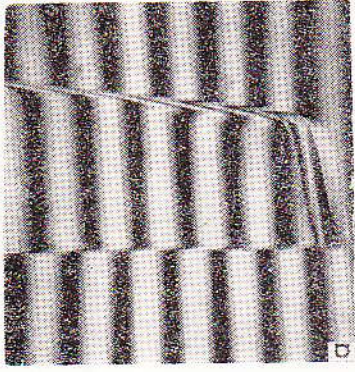


Fig. 57: Image of a birefringent cellophane strip as seen in a fringed interference field  
 a) Strip with its optical axis set at right angles to the direction of interference fringes; b, c) Strip with its optical axis in parallel and perpendicular alignment versus direction of light vibration in the polarizer (birefringent prism No. 2; X10 objective)

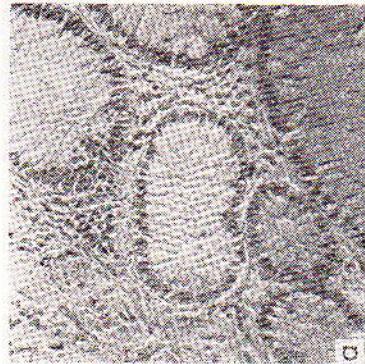
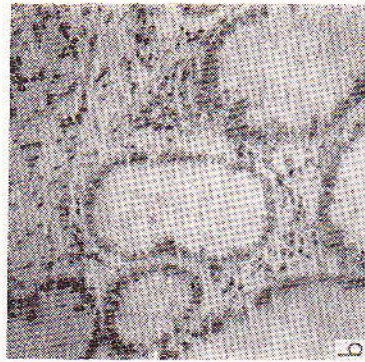


Fig. 56: Image of a histological preparation stained and sealed with the Canada balsam  
 a) As seen through a polarizing interference microscope in uniform differential field (birefringent prism No. 1); b) As seen through an ordinary bright field microscope (X20 objective)

ACCESSORIES and PARTS

1. EACH BIOLAR PI POLARIZING AND INTERFERENCE MICROSCOPE IS DELIVERED COMPLETE WITH THE FOLLOWING ITEMS:

It.	Description	Symbols		No. off
		literal	numerical	
1	Stand	B Zs 1	23080701	1
2	Interference head	UPI Zs 1	25520701	1
3	Centring substage	SK14 Zs 1	27090701	1
4	Eyepiece attachment	MND8 Zs 1	25120701	1
5	Condenser with slit	MPI 3 Zs 3	25510703	1
6	Polarizing interference condenser	KPI 2 Zs 1	26400701	1
7	Polarizer, enclosed	MPI 3 Zs 4	25510704	1
8	Multiple nosepiece	RO4 Zs 1	27500701	2
9	Achromatic X10 objective	Ob 103C Zs	3529	1
10	Achromatic X20 objective	Ob 203C Zs	3530	1
11	Achromatic X40 objective	Ob 404 Zs	3539	1
12	Achromatic X100 objective	Ob 1003C Zs	3532	1
13	Polarizing interference X10 objective	Ob 103 PI Zs	3720	1
14	Polarizing interference X20 objective	Ob 203PI Zs	3721	1
15	Polarizing interference X40 objective	Ob 403PI Zs	3722	1
16	Polarizing interference X100 objective	Ob 1003PI Zs	3723	1
17	Huyghenian X8 eyepiece	OK8H Zs 1	39310701	2
18	Wide field X10 eyepiece	OK10SK Zs 1	41200701	2
19	Orthoscopic X12.5 eyepiece	OK7a Zs 0	41300701	2
20	Measuring X12 eyepiece	OK12MO Zs 1	41380701	1
21	Auxiliary microscope	MPh Zs 1	26320701	1



Fig. 58: Image of diatom „Pleurosigma Angulatum“ as seen in an uniform interference field with birefringent prism  $W_2$  having different angular positions versus prism No. 3 ( $W_1$ )

a) Refracting edge in prism  $W_2$  forms an angle of 45 deg. with that of prism  $W_1$ ;  
 b) Direction of refracting angle  $\varphi_2$  in prism  $W_2$  is opposite versus this of refracting angle  $\varphi_1$  in prism  $W_1$ ; c) Direction of refracting angle  $\varphi_2$  in prism  $W_2$  being consistent with that of refracting angle  $\varphi_1$  in prism  $W_1$ . Total magnification about X200

2. UPI POLARIZING INTERFERENCE EQUIPMENT — ACCESSORIES

It.	Description	Symbols		No. off
		literal	numerical	
1	2	3	4	5
1	Interference head	UPI Zs 1	25520701	1
2	Condenser with slit	MPI 3 Zs 3	25510703	1
3	Polarizing interference condenser	KPI 2 Zs 1	26400701	1
4	Multiple nosepiece	RO4 Zs 1	27500701	1
5	Polarizing interference X10 objective	Ob 103 PI Zs	3720	1
6	Polarizing interference X20 objective	Ob 203 PI Zs	3721	1
7	Polarizing interference X40 objective	Ob 403 PI Zs	3722	1
8	Polarizing interference X100 objective	Ob1003 PI Zs	3723	1
9	Polarizer, enclosed	MPI 3 Zs 4	25510704	1
10	Measuring X12 eyepiece	OK12MO Zs 1	41380701	1
11	Auxiliary microscope	MPh Zs 1	26320701	1
12	Interference filter, 546 nm	Fi 546 Zs 1	28580701	1
13	Interference filter, 590 nm	Fi 590 Zs 1	28590701	1
14	Micrometric eyepiece plate 10/100	MOL 10/100 cz 1-01	28340101	1
15	Standard plate	PPI/100 Zs 1-01	28310001	1
16	Key	KPI 2 Zs 1-1	26400807	1
17	Condenser key	KF15 Zs 2	25860702	1
18	Soft brushes	ZN-57/MPC	0.9.07.0100	1
19	Flannel cloth IA No. 1	15-01090	0.9.08.0100	1
20	Container	ZN-57/MPC	15-01124	1
21	Technical description	UPI-F Zs	25520750	1
22	Guarantee card		23922980	1
			25522998	1

22	Interference filter, 546 nm	FI 546 Zs 1	28580701	1
23	Interference filter, 590 nm	FI 590 Zs 1	28590701	1
24	Blue filter	MB30 cz 1-05	23040105	1
25	Green filter	MB30 cz 1-06	23040106	1
26	Yellow filter	MB30 cz 1-07	23040107	1
27	Ground glass	M440 cz 1000	23110101	1
28	Micrometric eyepiece plate 10/100	MOL 10/100 cz 1-01	28340101	1
29	Lamp fitting	OS21 Zs 1	26790701	1
30	Lamp 6 V/15 W	OSRAM 8018	0.9.99.0029	5
31	Power supply unit	TM6/50	2926	1
32	Key	B Zs 4	23080704	1
33	Small key	KPI 2 Zs 1-7	26400807	1
34	Condenser key	KPI 5 Zs 2	25860702	1
35	Object micrometer	PPI/100 Zs 1-01	28310001	1
36	Jar filled with immersion oil	SOJ Zs	2874	1
37	Jar filled with XYLOR remover	SZX Zs	2875	1
38	Eyepiece tube cover	ON1 cz 1-1	41561001	2
39	Eye shell	MW1 cz 1-1	28001001	2
40	Soft brush	ZN-57(MPC)	0.9.07.0100	1
41	Flannel cloth IA No. 1	15-01090	0.9.08.0100	1
42	Container	ZN-57(MPC)	15-01124	1
43	Technical description	BP1-FZs	24920750	1
44	Guarantee card		23922980	1
			23922998	1

3. OUTFIT FOR A BIOLAR PI MICROSCOPE OR POLARIZING INTERFERENCE UPI EQUIPMENT — OPTIONAL ACCESSORIES

Description	Literal symbol	Numerical symbol	No.
Refractometric plates	PRF Zs	4154	1
Microscope attachment with a penumbra eyepiece (half-shade)	MNOP Zs	2487	1
Planachromatic X10 objective	Ob 108 Zs	3620	1
Planachromatic X20 objective	Ob 208 Zs	3627	1
Planachromatic X40 objective	Ob 408 Zs	3622	1
Planachromatic X100 objective	Ob 1008 Zs	3623	1
Plancompensating eyepiece X8	Ok 8 Pk Zsl	39780701	2
Plancompensating eyepiece X16	Ok 16 Pk Zsl	39790701	2
Microscope photographic attachment 6.5x9 cm	MNF Zs	2560	1
Microscope photographic attachment 24x36 mm	MNFA Zs	2566	1
Adaptor for EXACTA and VAREX cameras	MNF Zs 8	25600706	1
Adaptor for PRACTICA and CONTAX cameras	MNF Zs 10	25600707	1
Adaptor for LEICA and ZORKI cameras	MNF Zs 12	25600708	1
Halogen illuminator	OH Zs	2680	1
Microscope projector lens	MNP1 Zs	2541	1
Microscope drawing eyepiece	MOR Zs	2534	1
Monocular eyepiece	MNJ5 Zs	2490	1
Mechanical rotary stage	SO7 Zs	2717	1
Centring substage	NK6 Zs	2733	1

**Refractometric plates** (or slides) are designed to measure refractive index in liquids. For their construction and measuring procedure refer to Chapter 6 It. 4.

**Microscope penumbra eyepiece MNOP** has been designed to step up accuracy and to improve measurement technique of optical path difference when using uniform field method with a high image shearing effect. Optical path difference can in this case be measured with an almost twice as high accuracy as before, i.e. an accuracy of  $\lambda/500$ . For measurement procedure refer to Chapter 5 It. 2.

**Planachromatic objectives with compensating eyepieces** ensure that highest quality microscopic image can be achieved throughout the entire field of view. With the planachromatic objectives used on a BIOLAR PI microscope one can endeavour to carry out all the described measurements without producing an additional shearing effect. Planachromatic objectives must be ordered together with the compensating eyepieces.

**Microphotography equipment** enables miniature photographs of small objects for being taken on 6.5x9 cm glass plates, 6x9 cm cut films and 24x36 mm rolled films.

**MNF** — Photographic attachment for taking photographs of microscopic preparations on 6.5x9 cm plates or films.

Focusing process includes observation of image in the image sharpness setter (photographic attachment peep-hole). Exposure time represents a manual adjustment.

**MNFA** — Photographic attachment for taking photographs of microscopic preparations on 24x36 mm rolled films. Focusing and exposure time setting as the MNF item.

Both these attachments, and MNFA in the first place, are made available with the following adaptors for use with the cameras, as follows:

**EXACTA-VAREX:** adaptor MNF Zs 8

**PRACTICA & CONTAX:** adaptor MNF Zs 10

**LEICA and ZORKI:** adaptor MNF Zs 12

These adaptors are delivered as optional items of the MNF and MNFA equipment and for this reason they are supplied on customer's request packed separately so as to suit the type of camera owned by him.

**Halogen illuminator OH** with a halogen 100 W/12 V lamp can be used instead of a filament type illuminator when a stronger source of light is required, e.g. in microphotography, drawing and similar practices.

**Microscope projector lens MNP1** finds primarily use in didactics. With its aid several people can observe, at a time, one and the same microscopic image on a screen. Screen is 140 mm in diameter with X8 and X12.5 magnification of the lens itself.

Through the use of HO halogen illuminator adequate brightness can be adopted for the image being viewed.

**Microscope drawing eyepiece MOR** has been designed to enable contouring of objects viewed through the microscope with a simultaneous observation of the specimen and pencil end in motion.

Whenever required, an eyepiece micrometer can be inserted inside to measure the specimen. Eyepiece control is movable within a span such as to ensure dioptric adjustment from -4 to +3 diopters. Eyepiece magnification is X10.

MOR has been designed for use with only monocular MNJ5 eyepieces.

**Monocular eyepiece MNJ5** in the eyepiece tube axis can be swung back from vertical through an angle of 55 deg. Magnification  $\times 1$ .

**Mechanical rotary stage S07** has been designed for applications where a rotation of the stage through  $\pm\pi\cdot 360$  degrees and its accurate positioning in the desired angular setting are required. Especially suitable for polarized light examinations. The NK6 centring substage can be added to said stage, if necessary.

Two adjustment screws and keys are provided to enable axial alignment of the stage versus microscope centre line. Accuracy of angular readings — 0.1°. A ratchet device has been added to enable positioning of the upper plate every  $45 \pm 1$  degrees.

**Centring substage NK6** can be fitted on stage S07. It renders possible mechanical movement of the specimen in the mutually perpendicular directions within a range of  $25 \times 75$  mm.

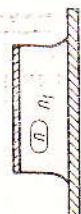


Table I

**INTERFERENCE COLOURS FOR OPTICAL PATH DIFFERENCES BETWEEN ORDINARY AND EXTRAORDINARY WAVES**

Optical path difference in nm	Polarizer and analyser crossed	Polarizer and analyser in parallel alignment
1	2	3
00	Black	White
40	Metallic grey	White
97	Lavender grey	Yellowish white
158	Greyish blue	Yellowish pale
218	Clearer grey	Yellow-brown
234	Greenish white	Brown
259	White	Bright red
267	Yellowish white	Carmine-red
275	Pale straw yellow	Red-brown
281	Straw yellow	Dark violet
306	Bright yellow	Indigo
332	Vivid yellow	Blue
430	Brown-yellow	Grey-blue
505	Red-orange	Bluish green
536	Warm red	Pale green
551	Deep red	Yellowish green
565	Purple	Bright green
575	Violet	Greenish yellow
589	Indigo	Golden yellow
664	Sky blue	Orange
728	Blue	Brown-orange
747	Greenish green	Carmine-red
826	Bright green	Bright purple
843	Yellowish green	Violet-purple
866	Greenish yellow	Violet
910	Clear yellow	Indigo
948	Vivid orange	Dark blue
998	Orange-red	Greenish blue
1101	Dark red	Green
1128	Violet-blue, bright	Yellowish green
1151	Indigo	Yellow-brown
1258	Greenish shade blue	Flesh colour
1334	Sea-green	Brown-red
1376	Brilliant green	Violet



Table III  
**KEY TO ESTIMATE REFRACTIVE INDEX OF MICRO-OBJECTS AND SURFACE IRREGULARITIES \*)**

SHAPE	REFRACTIVE INDEX	DIFFERENTIAL METHOD (PRISM No. 1)	UNIFORM FIELD METHOD WITH HIGH IMAGE SHEARING EFFECT (PRISM No. 3)	Peculiarity to identify method being used	
				Direction in which dark colour is being displaced	Sequence of extinction for images split
 or  (Hill)	$n > n_1$	Consistent with that of birefringent prism displacement	Consistent with the direction of birefringent prism displacement	LH image darkening on RH side of dark fringe whereas RH image on its LH side	
	$n < n_1$	Opposite versus that of birefringent prism displacement	Opposite versus that of birefringent prism displacement	LH image darkening on LH side of dark fringe whereas RH image on its RH side	
 (Valley)	$n > n_1$	Opposite versus that of birefringent prism displacement	Opposite versus that of birefringent prism displacement	LH image darkening on LH side of dark fringe whereas RH image on its RH side	
	$n < n_1$	Consistent with that of birefringent prism displacement	Consistent with the direction of birefringent prism displacement	LH image darkening on RH side of dark fringe whereas RH image on its LH side	

\*) NOTE: True for prisms  $W_1 W_2$  (Fig. 9) having an identical position and for prism  $W_3$  having a neutral position.

**BIBLIOGRAPHY**

1. Barer R.: Determination of dry mass, thickness, solid and water concentration in living cells. NATURE, vol. 172 (1953), p. 1087.
2. Barer R.: Interference microscopy and mass determination. NATURE, vol. 169 (1952), p. 336.
3. Barer R.: Refractometry and interferometry of living cells. Journ. Opt. Soc. Am., vol. 147 (1957), p. 545.
4. Barer R.; Dick D.A.T.: Interferometry and refractometry of cells in tissue culture in cytochemical methods with quantitative aims. Exp. Cell Res., Suppl., vol. 4 (1957), pp. 103—135. Academic Press Inc., New York (1957).
5. Chlap Z., Mirek T.: Utilisation en cytodagnostic du microscope interférentiel à polarisation pour déterminer la masse sèche des cellules. Revue Cytologie Clinique; vol. 2, No. 4 (1969), p. 23-2.
6. Darzynkiewicz Z., Jurkova Z., Więckowski J.: Interferometric measurements of the alkaline phosphatase activity in epithelial cell from the vagina of mice in the course of the keratinization process. Bull.Acad.Pol.Sci., vol. 13 (1956), p. 275.
7. Darzynkiewicz Z., Więckowski J.: Use of interference microscopy for quantitative estimation of alkalides phosphatase activity in Ehrlich ascites tumor cells. Folia Histochemica et Cytochemica. Vol. 3 (1965), p. 275.
8. Darzynkiewicz Z., Dokov V.K., Pieńkowski M.: Dry mass of lymphocytes during transformation after stimulation by phytohaemagglutinin. NATURE (London), vol. 214 (1967), pp. 1265—1266.
9. DeVies H.G., Deeley E.M.: An integrator for measuring the „dry mass” of cells and isolated components. Exp. Cell Res., vol. 11 (1956), pp. 169—185.
10. DeVies H.G., The determination of mass and concentration by microscope interferometry. General Cytochemical Methods, F.J. Danielli, Academic Press, New York (1958), p. 55.